ELSEVIER

Engineering Analysis with Boundary Elements 24 (2000) 549–557

ENGINEERING ANALYSIS *with* BOUNDARY ELEMENTS

www.elsevier.com/locate/enganabound

Solution of Poisson's equation by iterative DRBEM using compactly supported, positive definite radial basis function

A.H.-D. Cheng[a,*], D.-L. Young[b], C.-C. Tsai[b]

[a]*Department of Civil and Environmental Engineering, University of Delaware, Newark, DE 19716, USA*
[b]*Department of Civil Engineering, National Taiwan University, Taipei, Taiwan, R.O.C.*

Abstract

In the numerical solution of three-dimensional boundary value problems, the matrix size can be so large that it is beyond a computer's capacity to solve it. To overcome this difficulty, an iterative dual reciprocity boundary element method (DRBEM) is developed to solve Poisson's equation without the need of assembling a matrix. The DRBEM procedure requires that the right hand side of Poisson's equation be approximated by a radial basis function interpolation. In the iterative solution, it is found that only compactly supported, positive definite radial basis functions lead to converged results.

Keywords: Boundary element method; Dual reciprocity boundary element method; Radial basis function; Iterative method; Poisson's equation

1. Introduction

In the numerical solution of complex three-dimensional problems, a large number of discrete unknowns are required to accurately represent the geometry and the solution variation. When the matrix representing the linear or nonlinear system of equations is assembled, its size can be so large such that it poses difficulty for the computer to store it in the random access memory and to solve it by elimination. Consequently, the matrix size becomes the limiting factor that defines the largest problem a given computer can solve.

In the finite difference method (FDM), the need for assembling a solution matrix can be circumvented by using the so-called relaxation technique pioneered by Southwell [1,2]. To apply this technique, an initial trial solution is assigned to a solution grid. The discrete values at each node is corrected in an iterative manner, until convergence is achieved. No matrix or matrix solution is needed. Because of this advantage, large size fluid dynamic problems are typically solved by the finite difference method, not by the finite element method (FEM). It appears that this iterative solution idea can be extended to the boundary element method (BEM).

A search in the literature finds a number of BEM solutions that utilize iterative techniques [3–7]. However, matrices were assembled in those implementations. Iterative techniques were used only to invert the matrices. These methods do not meet our definition.

Iterative BEMs that do not assemble solution matrices do exist. To our knowledge, the first such attempt was made by Cahan, et al. [8] for solving Laplace's equation based on the direct BEM formulation. Later, an improved version was presented by Cahan and Lafe [9]. An iterative BEM based on the indirect formulation was devised for solving the governing equations of stochastic boundary value problems [10,11]. In those stochastic problems, not only the mean, but also the covariances are obtained. For a boundary geometry discretized into N nodes, the number of unknown covariances is N^2. The matrix, if assembled, would be of the size $N^2 \times N^2$. These unusually large sizes have necessitated the use of an iterative technique.

In this paper, we shall revisit the iterative BEM with the goal of solving Poisson's equation. The inhomogeneous right-hand side is treated by the dual reciprocity boundary element method (DRBEM) [12]. The underlying reason for the current practice is to construct an efficient algorithm to solve three-dimensional fluid dynamics problems governed by Navier–Stokes equations. By a velocity–vorticity formulation and a time-marching scheme, Navier–Stokes equations can be transformed into a number of Poisson's and Helmholtz-type equations. The iterative DRBEM can then be implemented for these equations. In this paper, however, only two-dimensional Poisson's equations are solved as a demonstration of the methodology.

* Corresponding author. Tel.: +1-302-831-2442; fax: +1-302-831-3640.
E-mail address: cheng@chaos.ce.udel.edu (A.H.-D. Cheng).

0955-7997/00/$ - see front matter
PII: S0955-7997(00)00035-7

As a part of the DRBEM solution process, the right hand side of Poisson's equation is approximated by an interpolation using radial basis functions. The coefficients of the interpolation are determined by collocation. Iterative methods are developed to avoid the assemblage of matrices. However, it is discovered that when conventional radial basis functions are used, none of the iterative methods tested converges. In fact, only the recently derived compactly supported, positive definite radial basis functions [13] can achieve convergence. These and other findings are reported in this paper.

2. Formulation of DRBEM

The governing equation investigated is Poisson's equation,

$$\nabla^2 \phi(\mathbf{x}) = f(\mathbf{x}) \tag{1}$$

In a DRBEM formulation, the right-hand side of Eq. (1) is interpolated using a combination of monomials and radial basis functions: [14]

$$f(\mathbf{x}) = \sum_{i=1}^{n_r} \alpha_i \varphi(r_i) + \sum_{i=1}^{n_p} \beta_i p_i(\mathbf{x}) \tag{2}$$

where $\varphi(r)$ is a radial basis function, $r_i = \|\mathbf{x}_i - \mathbf{x}\|$ is the Euclidean distance between a field point $\mathbf{x}$ and the ith collocation point $\mathbf{x}_i$, $p_i(\mathbf{x})$ is a multi-variate monomial, α_i and β_i are coefficients to be determined by collocation and constraint equations, n_r is the number of collocation nodes, and n_p is the number of monomial terms needed to support the convergence and stability of the approximation scheme [14]. The collocation nodes are distributed in the interior as well as on the boundary, hence their number is relatively large. α_i and β_i need to be solved from Eq. (2) prior to the implementation of the BEM. In addition, we need to find the particular solutions of the following Poisson's equations using the radial and monomial basis functions as the right hand side:

$$\nabla^2 \psi = \varphi(r) \tag{3}$$

$$\nabla^2 q_i = p_i; \qquad i = 1, \ldots, n_p \tag{4}$$

The analytical expressions for ψ and q_i can be found in the literature [14,15], hence is not repeated here. We shall return to more details of the RBF in Section 4.

Given a radial-basis-function interpolation, a 'boundary-only' integral equation that solves Poisson's Eq. (1) can be found as [12]

$$c(\mathbf{x})\phi(\mathbf{x}) = c(\mathbf{x})\left[\sum_{i=1}^{n_r} \alpha_i \psi(\mathbf{x} - \mathbf{x}_i) + \sum_{i=1}^{n_p} \beta_i q_i(\mathbf{x})\right] + \int_\Gamma G(\chi - \mathbf{x})\left[\frac{\partial \phi(\chi)}{\partial n(\chi)} - \sum_{i=1}^{n_r} \alpha_i \frac{\partial \psi(\chi - \mathbf{x}_i)}{\partial n(\chi)} - \sum_{i=1}^{n_p} \beta_i \frac{\partial q_i(\chi)}{\partial n(\chi)}\right] \mathrm{d}\chi - \oint_\Gamma \frac{\partial G(\chi - \mathbf{x})}{\partial n(\chi)}\left[\phi(\chi) - \sum_{i=1}^{n_r} \alpha_i \psi(\chi - \mathbf{x}_i) - \sum_{i=1}^{n_p} \beta_i q_i(\chi)\right] \mathrm{d}\chi \tag{5}$$

where $\mathbf{x}$ is the base point, $\chi \in \Gamma$ is a field point, $\mathbf{x}_i \in \Omega$ is a collocation point, Γ denotes the solution boundary, and Ω the solution domain, c is a geometric factor equal to 0, 1/2, or 1, depending on the location of $\mathbf{x}$, n is the outward normal direction of Γ, and G is the free-space Green's function given by

$$G = -\frac{\ln r}{2\pi} \tag{6}$$

for two-dimensional problems, with $r = \|\chi - \mathbf{x}\|$. We note that the second integral in Eq. (5) is strongly (Cauchy) singular when $\mathbf{x} \in \Gamma$, due to the presence of the kernel $\partial G/\partial n$. The integration is performed in the Cauchy principal value sense and is denoted by $\oint$.

We observe that Eq. (5) is in a natural form for an iteration procedure. Similar to the relaxation method, we can assign a set of initial trial values to all boundary nodes. We then apply Eq. (5) by placing the base point on a boundary node where ϕ is an unknown. Performing the integration and summation according to the right hand side of Eq. (5), we obtain an updated value of ϕ at that node. We then move on to the next node and repeat the procedure.

In a mixed boundary value problem, there exist nodes on which $\partial\phi/\partial n$, instead of ϕ, is the unknown. To have a formula for this situation, the dual integral equation approach [16] is taken. Eq. (5) can be differentiated at a boundary point $\mathbf{x} \in \Gamma$ in the direction of boundary normal n. The resultant equation is a hypersingular equation containing Hadamard finite part integrals denoted by $\oint\!\!\!\!=$:

$$c(\mathbf{x})\frac{\partial \phi(\mathbf{x})}{\partial n(\mathbf{x})} = c(\mathbf{x})\left[\sum_{i=1}^{n_r} \alpha_i \frac{\partial \psi(\mathbf{x} - \mathbf{x}_i)}{\partial n(\mathbf{x})} + \sum_{i=1}^{n_p} \beta_i \frac{\partial q_i(\mathbf{x})}{\partial n(\mathbf{x})}\right] + \int_\Gamma \frac{\partial G(\chi - \mathbf{x})}{\partial n(\mathbf{x})}\left[\frac{\partial \phi(\chi)}{\partial n(\chi)} - \sum_{i=1}^{n_r} \alpha_i \frac{\partial \psi(\chi - \mathbf{x}_i)}{\partial n(\chi)} - \sum_{i=1}^{n_p} \beta_i \frac{\partial q_i(\chi)}{\partial n(\chi)}\right] \mathrm{d}\chi - \oint\!\!\!\!= \int_\Gamma \frac{\partial^2 G(\chi - \mathbf{x})}{\partial n(\chi)\, \partial n(\mathbf{x})}\left[\phi(\chi) - \sum_{i=1}^{n_r} \alpha_i \psi(\chi - \mathbf{x}_i) - \sum_{i=1}^{n_p} \beta_i q_i(\chi)\right] \mathrm{d}\chi \tag{7}$$

The pair of integral Eqs. (5) and (7), can be alternately used in Neumann and Dirichlet type boundary conditions to update the missing boundary values. The process continues until convergence is reached.

The hypersingular Eq. (7), however, adds to the complexity of the solution. The hypersingularity needs to be regularized before its finite part can be evaluated. Several techniques exist [16]. In this paper we choose to avoid this issue by using only the Cauchy singular Eq. (5). To overcome the difficulty of solving mixed boundary value problems, the iterative scheme suggested by Cahan and Lafe [9] is adopted. Details of the method are presented in the next section.

3. Iterative scheme

To devise a scheme that uses only Eq. (5), we seek its discretized form, which can be expressed as follows:

$$\sum_{k=1}^{N} a_{jk}\phi^k - \sum_{k=1}^{N} b_{jk}\phi_n^k = c_j, \qquad j = 1,\ldots,N \tag{8}$$

where ϕ^k is the discrete value of ϕ at node k, ϕ_n^k is the discrete value of $\partial\phi/\partial n$ at node k, coefficients a_{jk}, b_{jk}, and c_j are constants obtained by integration over the elements. Given either a Dirichlet or a Neumann type condition, we can extract the corresponding unknown variable $\partial\phi/\partial n$ and ϕ, respectively, to form the following iterative formulae

$$\phi_n^j = \frac{1}{b_{jj}}\left[-c_j + \sum_{k=1}^{N} a_{jk}\phi^k - \sum_{\substack{k=1\\k\neq j}}^{N} b_{jk}\phi_n^k\right], \qquad \text{if } \phi^j \text{ is given} \tag{9}$$

$$\phi^j = \frac{1}{a_{jj}}\left[c_j - \sum_{\substack{k=1\\k\neq j}}^{N} a_{jk}\phi^k - \sum_{k=1}^{N} b_{jk}\phi_n^k\right], \qquad \text{if } \phi_n^j \text{ is given} \tag{10}$$

Hence the pair of Eqs. (9) and (10) forms the basis of an iterative scheme. Particularly, a procedure similar to the Gauss–Seidel scheme, in which an updated datum is immediately put into use in the evaluation of next datum, can be applied.

The above equations differ from a typical FDM relaxation formula in that the solution at a given node is dependent on values on all nodes of the boundary, not just a few neighboring nodes. An advantage of this property is that in the summation of Eqs. (9) and (10) half of the data are already correct, supplied by the known boundary conditions. This allows zero initial trial values be assigned to all the unknowns. The first correction can already bring the solution into a reasonable range of the true solution. Hence a stable scheme is expected.

In a standard BEM, Eqs. (9) and (10) are assembled into a matrix system

$$[\mathbf{A}]\{\mathbf{x}\} = \{\mathbf{b}\} \tag{11}$$

where $[\mathbf{A}]$ is an $N \times N$ matrix. In the current iterative scheme, $[\mathbf{A}]$ is not assembled. Its elements are calculated on the fly and immediately discarded. Hence only column matrices of size N are needed. We also notice that all quantities under the summation signs in Eqs. (5) and (6) are known quantities that do not change from iteration to iteration. These parts are computed only once and stored in an array of size N.

The need for regenerating elements in the coefficient matrix over and over is a major disadvantage of the iterative method as the cost of numerical integration can be high. This problem is alleviated by the use of low-order elements, over which exact integration is available. For the current implementation, constant elements and their exact integrations are used. Hence the cost of integration is minimized.

4. Radial basis functions

The theoretical basis of radial basis function (RBF) and its application in DRBEM have been well explored by Golberg, Chen, and co-workers in a series of articles. See, for example, Golberg et al. [14] for a recent review. There exist a number of RBFs, such as the conical, spline, Gaussian, and multiquadric types. The conical type is given by

$$\varphi(r) = r^{2n-1}, \qquad n = 1,2,3,\ldots \tag{12}$$

The polyharmonic spline functions typically give better performance [17] and are given by

$$\varphi(r) = r^{2n}\ln r, \qquad n = 1,2,3,\ldots \tag{13}$$

The case $n = 1$ is known as the thin-plate spline. As indicated in Eq. (2), these RBFs need to be supplemented by a monomial family

$$p_i = \{1, x, y, x^2, y^2, xy, x^3, \ldots\} \tag{14}$$

to ensure proper convergence and stability of the scheme. Take for example, for the thin-plate spline $r^2 \ln r$, terms up to linear order, $\{1, x, y\}$, need to be included. For higher order splines $r^{2n}\ln r$, terms up to nth order must be incorporated.

The interpolation of the function $f(\mathbf{x})$ in Eq. (2) is accomplished by solving a set of collocation equations

$$\sum_{i=1}^{n_r} \alpha_i \varphi(r_{ij}) + \sum_{i=1}^{n_p} \beta_i p_i(\mathbf{x}_j) = f(\mathbf{x}_j), \qquad j = 1,2,\ldots,n_r \tag{15}$$

where $r_{ij} = \|\mathbf{x}_i - \mathbf{x}_j\|$, n_r is the number of collocation nodes, and n_p is the number of monomial terms needed. To determine the additional coefficients associated with the monomial terms, the following constraint equations are imposed:

$$\sum_{i=1}^{n_r} \alpha_i p_j(\mathbf{x}_i) = 0, \qquad \text{for } j = 1,2,\ldots,n_p \tag{16}$$

Eqs. (15) and (16) form a linear system of $n_r + n_p$ equations, solving for the $n_r + n_p$ unknowns, α_i and β_i. As

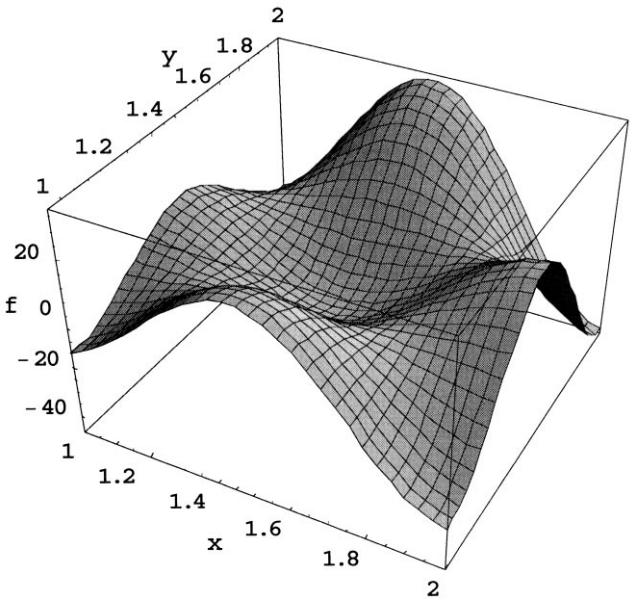

Fig. 1. The right hand side of Poisson's Eq. (23).

mentioned above, the number of monomial terms needed is dependent on the order of the RBF.

In an iterative scheme, the matrix corresponding to the linear systems (15) and (16) is not assembled. The matrix elements given as $\varphi(r_{ij})$, 1, x_i, y_i, etc. are instantly generated. Because of their simple form, the computation time is minimal.

Several standard iterative techniques, such as the Gauss–Seidel method and the conjugate gradient method, have been employed to perform the iteration. However, to our surprise, none of the iterative schemes worked! Replacing the RBF from spline types to conical types makes no difference. For the Gauss–Seidel method, a check of convergence condition shows that the spectral radius is greater than 1, hence the solution diverges as expected. For the conjugate gradient method, a check of the matrices shows that they are not positive definite. Convergence is not guaranteed.

Indeed, as commented by Chen, et al. [18] all of the above-mentioned RBFs are globally defined. The resulting interpolation matrix is dense and can be highly ill-conditioned, especially for a large number of interpolation points. This can cause serious stability problems. It was suggested [19] that the difficulty can be overcome by the use of a compactly supported, positive definite RBF (CS-PD-RBF) [13].

CS-PD-RBFs became available only recently. It was demonstrated by Wendland [13] that for a given dimension d and smoothness C^{2k}, a positive definite radial basis function in the form of a univariate polynomial of minimal degree always exists, and is unique within a constant factor. Results were given for $d = 1, 3, 5$. For the current two-dimensional problems, we choose two of the CS-PD-RBFs [13,18]: for $d = 3$ and $k = 0$

$$\varphi(r)\begin{cases}\left(1-\dfrac{r}{a}\right)^2, & \text{for } 0 \le r \le a\\ 0, & \text{for } r > a\end{cases} \tag{17}$$

and for $d = 3$ and $k = 1$

$$\varphi(r)\begin{cases}\left(1-\dfrac{r}{a}\right)^4\left(1+\dfrac{4r}{a}\right), & \text{for } 0 \le r \le a\\ 0, & \text{for } r > a.\end{cases} \tag{18}$$

Although $d = 3$ is used in the above, the corresponding CS-PD-RBF is valid for any lower dimension, which is a consequence of positive definiteness. Hence they are valid for the current two-dimensional problems. In the above, a is an influence radius beyond which the function is truncated to zero. The influence radius controls the density of the matrix. If a is larger than the largest span of the domain, the matrix is fully populated. If a is smaller than the smallest distance between two collocation nodes, the matrix becomes diagonal. A proper a value should fall between these two limits.

The interpolation equation for CS-PD-RBF is given by

$$f(\mathbf{x}) = \sum_{i=1}^{n_r} \alpha_i \varphi(r_i) \tag{19}$$

As compared to Eq. (15), we notice that polynomial terms are not needed for the CS-PD-RBF, for its positive definiteness. The coefficients α_i are determined from the collocation equations

$$\sum_{i=1}^{n_r} \alpha_i \varphi(r_{ij}) = f(\mathbf{x}_j), \qquad j = 1, 2, \ldots, n_r \tag{20}$$

The implementation of an iterative scheme solving the above system will be discussed in Section 5.

For the purpose of DRBEM implementation, the particular solution satisfying Eq. (3) with the CS-PD-RBF as the right hand side is needed. This has been found by Chen, et al. [18] The particular solution corresponding to Eq. (17) is

$$\psi = \begin{cases}\dfrac{r^2}{4} - \dfrac{2r^3}{9a} + \dfrac{r^4}{16a^2}, & \text{for } 0 \le r \le a\\ \dfrac{13a^2}{144} + \dfrac{a^2}{12}\ln\left(\dfrac{r}{a}\right), & \text{for } r > a.\end{cases} \tag{21}$$

In the second line of the above equation, we have corrected an error that exists (see Table 2 in Ref. [18]). For Eq. (18), the corresponding particular solution is

$$\psi = \begin{cases}\dfrac{r^2}{4} - \dfrac{5r^4}{8a^2} + \dfrac{4r^5}{5a^3} - \dfrac{5r^6}{12a^4} + \dfrac{4r^7}{49a^5}, & \text{for } 0 \le r \le a\\ \dfrac{529a^2}{5880} + \dfrac{a^2}{14}\ln\left(\dfrac{r}{a}\right), & \text{for } r > a\end{cases} \tag{22}$$

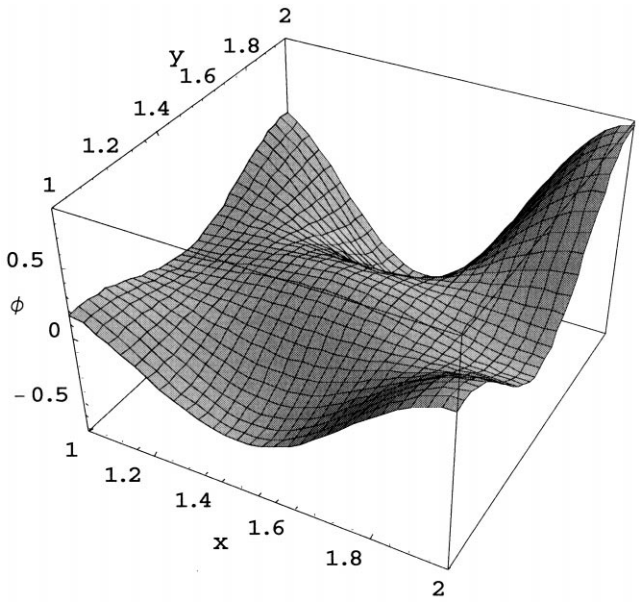

Fig. 2. The solution of Poisson's Eq. (23).

5. Example

To test the algorithm, an example with a known exact solution is investigated [15]. The problem is governed by the following Poisson's equation

$$\nabla^2\phi = -\frac{751\pi^2}{144}\sin\frac{\pi x}{6}\sin\frac{7\pi x}{4}\sin\frac{3\pi y}{4}\sin\frac{5\pi y}{4} + \frac{7\pi^2}{12}\cos\frac{\pi x}{6}\cos\frac{7\pi x}{4}\sin\frac{3\pi y}{4}\sin\frac{5\pi y}{4} + \frac{15\pi^2}{8}\sin\frac{\pi x}{6}\sin\frac{7\pi x}{4}\cos\frac{3\pi y}{4}\cos\frac{5\pi y}{4} \quad (23)$$

in the domain of $1 \le x \le 2$ and $1 \le y \le 2$. The right hand side function is plotted in Fig. 1. We observe that it has a relatively large variability. Eq. (23) is subject to the boundary conditions

$$\begin{aligned}
\phi(x,1) &= -\frac{1}{2}\sin\frac{\pi x}{6}\sin\frac{7\pi x}{4}\\
\phi(1,y) &= -\frac{1}{2\sqrt{2}}\sin\frac{3\pi y}{4}\sin\frac{5\pi y}{4}\\
\phi(x,2) &= -\sin\frac{\pi x}{6}\sin\frac{7\pi x}{4}\\
\phi(2,y) &= -\frac{\sqrt{3}}{2}\sin\frac{3\pi y}{4}\sin\frac{5\pi y}{4}
\end{aligned} \quad (24)$$

The exact solution of this problems is

$$\phi = \sin\frac{\pi x}{6}\sin\frac{7\pi x}{4}\sin\frac{3\pi y}{4}\sin\frac{5\pi y}{4} \quad (25)$$

which is plotted as Fig. 2.

The first step of solving this boundary value problem by DRBEM is to approximate the right hand side by a RBF interpolation. A uniform grid of 11×11 is laid over the domain for collocation. For the iterative solution of the linear system (20), a subroutine *linbcg* found in *Numerical Recipes* [20], based on the iterative bi-conjugate gradient method, is used. The subroutine requires a user-supplied matrix in compacted form. Since the present method does not assemble a matrix, the subroutine needs to be modified. This is easily accomplished by changing a few lines in the subroutine *atimes*, which performs matrix multiplication, called by subroutine *lincbg*.

The iterative method requires an initialization of the solution. By noticing that the diagonal terms of the CS-PD-RBF collocation matrix are all equal to unity, we can simply assign the initial trial values as

$$\alpha_i = f(\mathbf{x}_i), \qquad i = 1, 2, \ldots, n_r \quad (26)$$

For the influence radius, two cases are chosen: $a = 0.5$ and 1.5, which cover about 35 and 100% of the maximum linear dimension of the solution domain, respectively. The first-order CS-PD-RBF defined in Eq. (17) is adopted. The solution converges rapidly. For the case of $a = 0.5$, it takes 8 iterations for the solution to converge to a relative tolerance of 10^{-2}, and 17 iterations to a tolerance of 10^{-4}. The iterative scheme is highly efficient.

To investigate the effect of the influence radius and the order of CS-PD-RBF on the rate of convergence, cases are run with different combinations of these factors. The result is presented in Fig. 3. The two lower curves correspond to the first-order CS-PD-RBF defined in Eq. (17). It shows that the use of a larger influence radius that produces a full matrix only slightly increases the number of iterations. The upper two curves correspond to the second-order CS-PD-RBF defined in Eq. (18). The number of iterations has significantly increased, particularly for the larger influence radius case.

We next investigate the effect of the number of nodes, i.e. the size of the system, on the convergence rate. The results presented so far are based on an 11×11 mesh. We now vary the mesh size. The first-order CS-PD-RBF with the influence radius 0.5 is used in these cases. The tolerance is fixed at 10^{-3}. Fig. 4 plots the number of iterations versus the number of collocation nodes in log–log scale. The result indicates a relation

$$\text{iteration number} \sim \text{node number}^{1/2} \quad (27)$$

This convergence rate is the same as the successive-over-relaxation (SOR) method of the FDM [20].

The accuracy of the approximation is examined next. We plot in Fig. 5 the relative error, defined as the error normalized by the maximum absolute value of the solution, using the 11×11 grid and the first-order CS-PD-RBF with $a = 0.5$. The maximum error is found to be 2.8%, located near the corner (2,2). If we use the second-order CS-PD-RBF, the accuracy is only slightly improved, with a maximum error of -2.5%. If the influence radius for the first-order

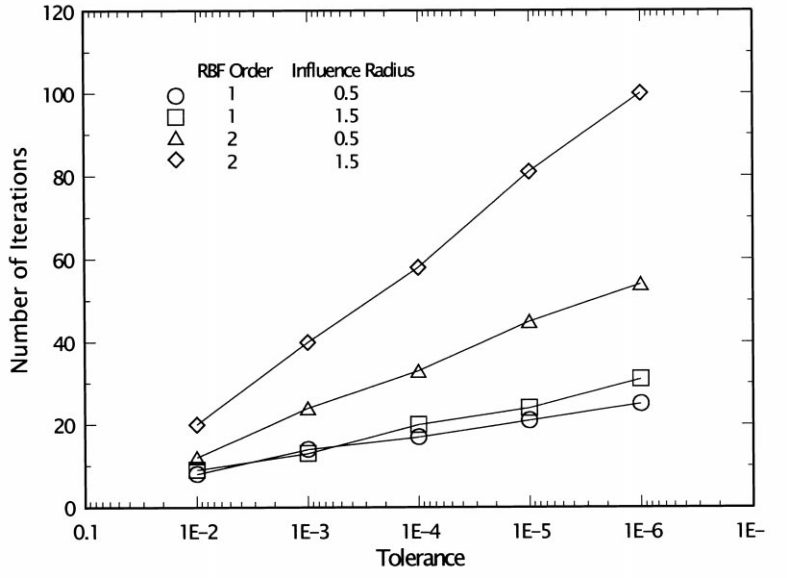

Fig. 3. Iterations needed for solution convergence as a function of tolerance, for different order CS-PD-RBFs and different scaling factors.

CS-PD-RBF is increased to $a = 1.5$, we also see very little improvement, with a maximum error of 2.5% observed. Judging from the performance of accuracy and efficiency, the first-order CS-PD-RBF with $a = 0.5$ will be used in the BEM solution below.

To compare the accuracy of the CS-PD-RBF with other RBFs, the same function on the right hand side of Eq. (23) was approximated by the thin-plate spline RBF using the same 11×11 collocation nodes. Fig. 6 shows the relative error. We observe that the thin-plate spline RBF, which gives an maximum error of 1.7%, performs better. The same case is also tested for the first-order conical RBF. The maximum error is around 2.6%, comparable to the CS-PD-RBF case. We should comment, however, that both the spline and the conical RBF collocations diverge in the iterative procedure, and have to be obtained by matrix elimination.

The next step is to find the BEM solution using the iterative procedure described in Section 3. The solution boundary is subdivided into 40 constant elements (nodes) with 10 on each side. The 11×11 collocation mesh is used for RBF interpolation. Fig. 7 plot the relative error of the solution. The maximum error is found to be 2%.

It is of interest to examine the rate of convergence of the iterative DRBEM under different element sizes and accuracy requirements. The problem is solved using four

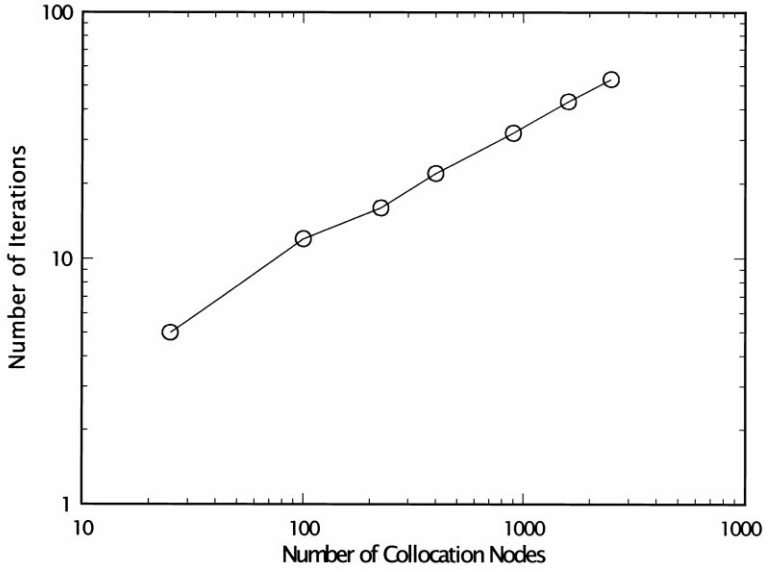

Fig. 4. Number of iterations as a function of the number of collocation nodes.

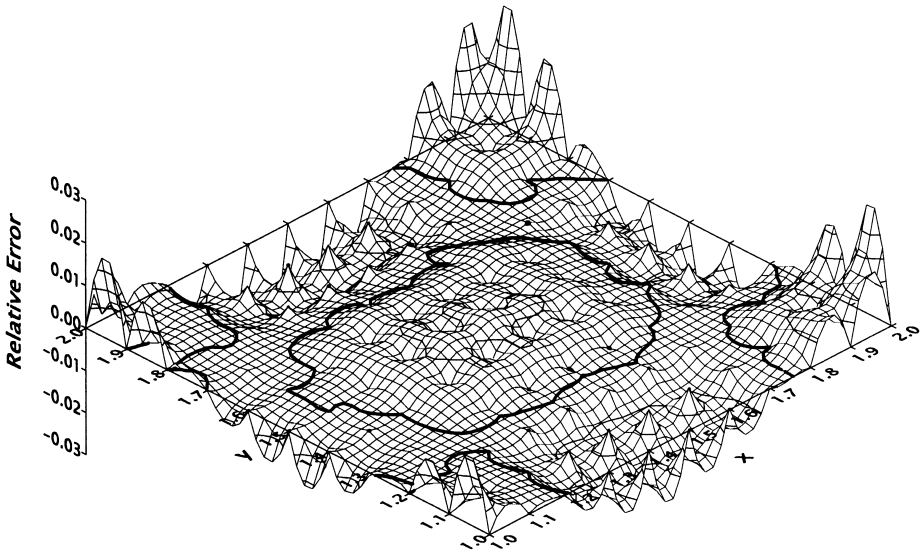

Fig. 5. Relative error of a first-order CS-PD-RBF interpolation. Thick contour lines mark zero error.

different meshes, involving 20, 40, 80, and 160 constant elements. A relative tolerance is defined as

$$\text{tol} = \max\left\{\left|\frac{\text{solution at iteration } \ell - \text{solution at iteration } \ell + 1}{\text{solution at iteration } \ell}\right|\right\} \tag{28}$$

Fig. 8 plots the number of iterations needed for the solution to converge to a specified tolerance versus the number of nodes, in log–log scale. We observe the relation

$$\text{iteration number} \sim \text{node number}^{3/4} \tag{29}$$

This rate of convergence is better than that of the Gauss–Seidel iterative scheme used in FDM, which has a rate proportional to the first power of the node number. It is however, worse than the SOR scheme, which converges at the rate of 1/2 power. We note that the current scheme is not accelerated, hence is equivalent to a Gauss–Seidel scheme. Acceleration should further improve the efficiency of the scheme. Furthermore, we should note that the comparison of efficiency with FDM is made with node number, not mesh size. As the linear dimension of the element size decreases, the node number for the BEM increases linearly for two dimensional problems. For the FDM, the node number increases by a power of 2. Hence the BEM should be highly competitive in solving large size problems.

Fig. 9 presents the number of iterations versus tolerance, in semi-log scale. The relation is roughly a straight line, suggesting

$$\text{iteration number} \sim \log(\text{tol}) \tag{30}$$

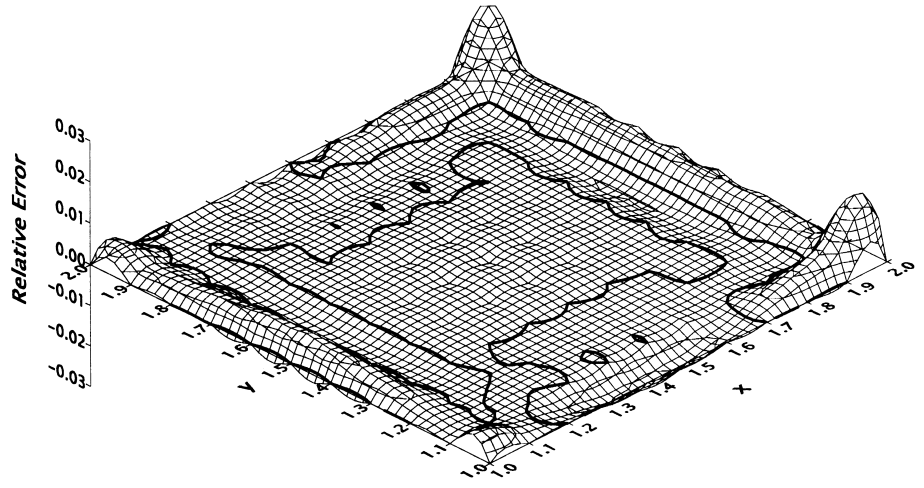

Fig. 6. Relative error of a thin-plate spline RBF interpolation. Thick contour lines mark zero error.

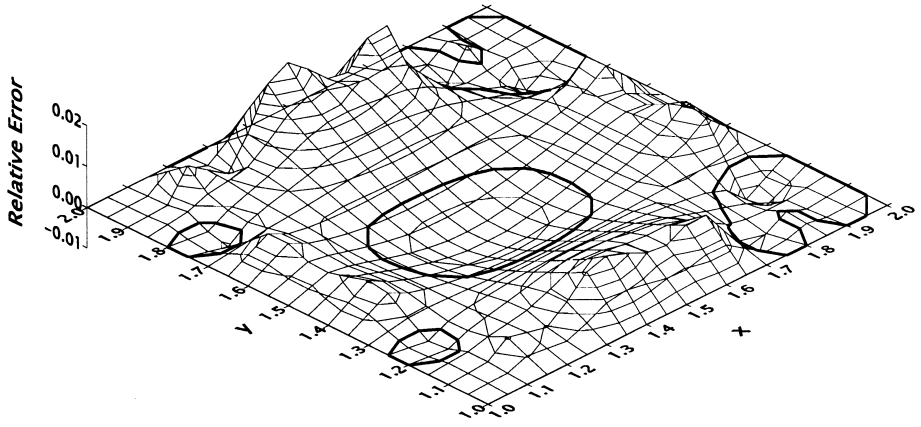

Fig. 7. Relative error of the boundary element solution. Thick contour lines mark zero error.

This behavior is the same as the Gauss–Seidel and the SOR schemes.

6. Conclusions

We have conducted a preliminary study in which an iterative DRBEM is constructed to solve problems governed by Poisson's equations. In the application of DRBEM, there are two linear systems to be solved — one involves the RBF interpolation of the right hand side of the Poisson's equation, and the other concerns the boundary integral equation solution. For both systems, they are solved by iterative schemes that do not assemble solution matrix. In the case of the collocation system for the RBF interpolation, it is found that only the compactly supported, positive definite radial basis functions lead to converged results. The accuracy and the convergence rate are investigated and compared with other methods. Although only a two-dimensional problem is solved in the current effort, the findings clearly indicate that the iterative DRBEM is a promising technique for solving large-size three-dimensional problems. This part of study, particularly relating to the solution of Navier–Stokes equations, is underway.

Acknowledgements

The work reported herein is supported by the National Science Council of the Republic of China (Taiwan), Grant no. NSC 88-2811-E-002-0008, during the first author's sabbatical leave at the National Taiwan University. The discussion with Michael Golberg and C.S. Chen brought our attention to the existence of the CS-PD-RBF. Their assistance is deeply appreciated.

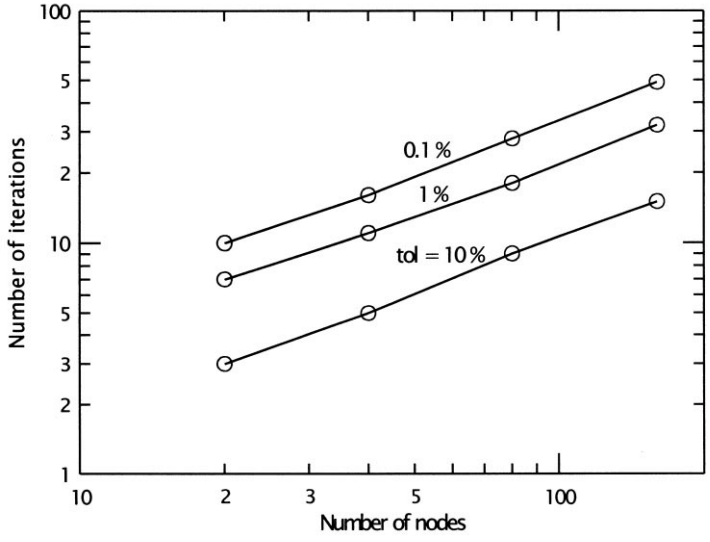

Fig. 8. Convergence rate shown as the number of iterations versus the number of nodes.

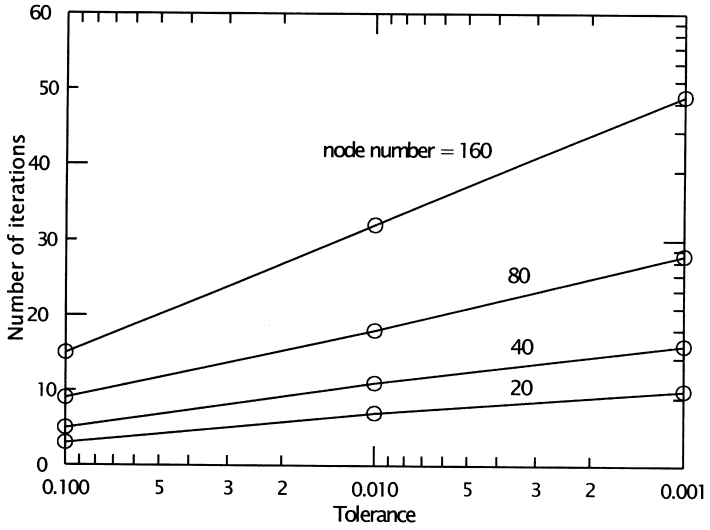

Fig. 9. Convergence rate shown as the number of iterations versus tolerance.

References

[1] Southwell RV. Relaxation methods in engineering science, A treatise on approximate computation. Oxford: Oxford University Press, 1940.
[2] Southwell RV. Relaxation methods in theoretical physics. Oxford University Press, 1946.
[3] Yang LS, Machidori H, Shirakawa T. BEM and BEM with SOR on the parallel computer QCDPAX. Engng Anal Bound Elem 1996;18:231–7.
[4] Lesnic D, Elliott L, Ingham DB. An iterative boundary element method for solving numerically the Cauchy problem for the Laplace equation. Engng Anal Bound Elem 1997;20:123–33.
[5] Mai-Duy N, Nguyen-Hong P, Tran-Cong T. A fast convergent iterative boundary element method on PVM cluster. Engng Anal Bound Elem 1998;22:307–16.
[6] Merkel M, Bulgakov V, Bialecki R, Kuhn G. Iterative solution of large-scale 3D-BEM industrial problems. Engng Anal Bound Elem 1998;22:183–97.
[7] Valente FP, Pina HLG. Iterative solvers for BEM algebraic systems of equations. Engng Anal Bound Elem 1998;22:117–24.
[8] Cahan BD, Scherson D, Reid MA. I-BIEM. An iterative boundary integral equation method for computer solutions of current distribution problems with complex boundaries-A new algorithm. J Electrochem Soc 1988;135:285–93.
[9] Cahan BD, Lafe OE. On the iterative boundary element method. In: Cheng AH-D, Brebbia CA, Grilli S, editors. Computational engineering with boundary elements, 2: solid and computational problems, Computational Mechanics, 1990. p. 199–209 BETECH90, University of Delaware.
[10] Cheng AH-D, Lafe OE. Boundary element solution for stochastic groundwater flow: random boundary condition and recharge. Water Resour Res 1991;27:231–42.
[11] Cheng AH-D, Abousleiman Y, Ruan F, Lafe OE. Boundary element solution for stochastic groundwater flow:temporal weakly stationary problems. Water Resour Res 1993;29:2893–908.
[12] Partridge PW, Brebbia CA, Wrobel LC. The dual reciprocity boundary element method. Amsterdam: CMP/Elsevier, 1992.
[13] Wendland H. Piecewise polynomial, positive definite and compactly supported radial functions of minimal degree. Adv Comput Math 1995;4:389–96.
[14] Golberg MA, Chen CS, Bowman H. Some recent results and proposals for the use of radial basis functions in the BEM. Engng Anal Bound Elem 1999;23:285–96.
[15] Cheng AH-D, Lafe O, Grilli S. Dual reciprocity BEM based on global interpolation functions. Engng Anal Bound Elem 1994;13:303–11.
[16] Chen JT, Hong H-K. Review of dual boundary element methods with emphasis on hypersingular integrals and divergent series. Appl Mech Rev, ASME 1999;52:17–33.
[17] Partridge P.W. Towards criteria for selection approximation functions in the Dual Reciprocity Method. Engng Anal Bound Elem 2000;24:519–29.
[18] Chen CS, Brebbia CA, Power H. Dual reciprocity method using compactly supported radial basis functions. Commun Numer Meth Engng 1999;15:137–50.
[19] Golberg MA, Chen CS. Private communication, 1999.
[20] Press WH, Teukolsky SA, Vetterling WT, Flannery BP. Numerical recipes in Fortran, the art of scientific computing. 2nd ed. Cambridge: Cambridge University Press, 1992.